

## Ibrutinib treatment ameliorates murine chronic graft-versus-host disease

Jason A. Dubovsky, ... , John C. Byrd, Bruce R. Blazar

*J Clin Invest.* 2014;124(11):4867-4876. <https://doi.org/10.1172/JCI75328>.

Research Article

Immunology

Chronic graft-versus-host disease (cGVHD) is a life-threatening impediment to allogeneic hematopoietic stem cell transplantation, and current therapies do not completely prevent and/or treat cGVHD. CD4<sup>+</sup> T cells and B cells mediate cGVHD; therefore, targeting these populations may inhibit cGVHD pathogenesis. Ibrutinib is an FDA-approved irreversible inhibitor of Bruton's tyrosine kinase (BTK) and IL-2 inducible T cell kinase (ITK) that targets Th2 cells and B cells and produces durable remissions in B cell malignancies with minimal toxicity. Here, we evaluated whether ibrutinib could reverse established cGVHD in 2 complementary murine models, a model interrogating T cell-driven sclerodermatous cGVHD and an alloantibody-driven multiorgan system cGVHD model that induces bronchiolar obliterans (BO). In the T cell-mediated sclerodermatous cGVHD model, ibrutinib treatment delayed progression, improved survival, and ameliorated clinical and pathological manifestations. In the alloantibody-driven cGVHD model, ibrutinib treatment restored pulmonary function and reduced germinal center reactions and tissue immunoglobulin deposition. Animals lacking BTK and ITK did not develop cGVHD, indicating that these molecules are critical to cGVHD development. Furthermore, ibrutinib treatment reduced activation of T and B cells from patients with active cGVHD. Our data demonstrate that B cells and T cells drive cGVHD and suggest that ibrutinib has potential as a therapeutic agent, warranting consideration for cGVHD clinical trials.

Find the latest version:

<https://jci.me/75328/pdf>



# Ibrutinib treatment ameliorates murine chronic graft-versus-host disease

Jason A. Dubovsky,<sup>1</sup> Ryan Flynn,<sup>2</sup> Jing Du,<sup>2</sup> Bonnie K. Harrington,<sup>3</sup> Yiming Zhong,<sup>1</sup> Benjamin Kaffenberger,<sup>1</sup> Carrie Yang,<sup>1</sup> William H. Towns,<sup>1</sup> Amy Lehman,<sup>1</sup> Amy J. Johnson,<sup>1</sup> Natarajan Muthusamy,<sup>1</sup> Steven M. Devine,<sup>1</sup> Samantha Jaglowski,<sup>1</sup> Jonathan S. Serody,<sup>4</sup> William J. Murphy,<sup>5</sup> David H. Munn,<sup>6</sup> Leo Luznik,<sup>7</sup> Geoffrey R. Hill,<sup>8</sup> Henry K. Wong,<sup>1</sup> Kelli K.P. MacDonald,<sup>8</sup> Ivan Maillard,<sup>9</sup> John Koreth,<sup>10</sup> Laurence Elias,<sup>11</sup> Corey Cutler,<sup>10</sup> Robert J. Soiffer,<sup>10</sup> Joseph H. Antin,<sup>10</sup> Jerome Ritz,<sup>10</sup> Angela Panoskaltsis-Mortari,<sup>2</sup> John C. Byrd,<sup>1</sup> and Bruce R. Blazar<sup>2</sup>

<sup>1</sup>Division of Hematology, Department of Internal Medicine, The Ohio State University, Columbus, Ohio, USA. <sup>2</sup>Masonic Cancer Center and Department of Pediatrics, Division of Blood and Marrow

Transplantation, University of Minnesota, Minneapolis, Minnesota, USA. <sup>3</sup>College of Veterinary Medicine, Veterinary and Comparative Medicine, The Ohio State University, Columbus, Ohio, USA.

<sup>4</sup>Lineberger Comprehensive Cancer Center, University of North Carolina School of Medicine, Chapel Hill, North Carolina, USA. <sup>5</sup>Department of Dermatology, University of California–Davis Cancer Center and

School of Medicine, Sacramento, California, USA. <sup>6</sup>Department of Pediatrics, School of Medicine, Medical College of Georgia, Augusta, Georgia, USA. <sup>7</sup>Sidney Kimmel Comprehensive Cancer Center and

Department of Oncology, Johns Hopkins University School of Medicine, Baltimore, Maryland, USA. <sup>8</sup>Queensland Institute of Medical Research Berghofer Medical Research Institute, Brisbane,

Queensland, Australia. <sup>9</sup>Life Sciences Institute, University of Michigan, Ann Arbor, Michigan, USA. <sup>10</sup>Department of Medical Oncology, Dana-Farber Cancer Institute,

Boston, Massachusetts, USA. <sup>11</sup>Pharmacyclis Inc., Sunnyvale, California, USA.

**Chronic graft-versus-host disease (cGVHD) is a life-threatening impediment to allogeneic hematopoietic stem cell transplantation, and current therapies do not completely prevent and/or treat cGVHD. CD4<sup>+</sup> T cells and B cells mediate cGVHD; therefore, targeting these populations may inhibit cGVHD pathogenesis. Ibrutinib is an FDA-approved irreversible inhibitor of Bruton's tyrosine kinase (BTK) and IL-2 inducible T cell kinase (ITK) that targets Th2 cells and B cells and produces durable remissions in B cell malignancies with minimal toxicity. Here, we evaluated whether ibrutinib could reverse established cGVHD in 2 complementary murine models, a model interrogating T cell-driven sclerodermatous cGVHD and an alloantibody-driven multiorgan system cGVHD model that induces bronchiolar obliterans (BO). In the T cell-mediated sclerodermatous cGVHD model, ibrutinib treatment delayed progression, improved survival, and ameliorated clinical and pathological manifestations. In the alloantibody-driven cGVHD model, ibrutinib treatment restored pulmonary function and reduced germinal center reactions and tissue immunoglobulin deposition. Animals lacking BTK and ITK did not develop cGVHD, indicating that these molecules are critical to cGVHD development. Furthermore, ibrutinib treatment reduced activation of T and B cells from patients with active cGVHD. Our data demonstrate that B cells and T cells drive cGVHD and suggest that ibrutinib has potential as a therapeutic agent, warranting consideration for cGVHD clinical trials.**

## Introduction

Chronic graft-versus-host disease (cGVHD) is a primary cause of nonrelapse mortality after allogeneic hematopoietic stem cell transplantation (HSCT) (1–4). Drug therapy for cGVHD has been predominantly limited to steroids and calcineurin inhibitors, which are incompletely effective and associated with infections as well as long-term risks of toxicity (5). Novel therapeutics that

pinpoint pathogenic immune subsets might control cGVHD yet preserve immune effector functions.

In contrast to acute GVHD, cGVHD is a relatively acellular process that has fibrosis as a dominant feature. The specific immune phenomena that underlie cGVHD are variable; however, recent studies show that B cells, in addition to specific CD4<sup>+</sup> T cell subsets, are key mediators of cGVHD (6–8). It has been demonstrated that pathogenic antibody deposition occurs in human cGVHD (9–12). A network of alloreactive T helper cells, including Th1, Th2, Th17, and T follicular helper (Tfh) cells, infiltrate tissues and produce a milieu of effector cytokines resulting in antibody deposition, tissue fibrosis, and autoimmunity (6, 8, 13–15).

Many of the cellular activation and effector functions of these lymphoid subsets can be molecularly tethered to Bruton's tyrosine kinase (BTK) and IL-2 inducible T cell kinase (ITK) (16, 17). BTK and ITK are highly conserved Tec family kinases that propagate immune receptor-based signaling in B and T lymphocytes, respectively (16). These molecules are activated upstream by SRC family kinases and, upon autophosphorylation, drive downstream acti-

**Authorship note:** Jason A. Dubovsky, Ryan Flynn, John C. Byrd, and Bruce R. Blazar contributed equally to this work.

**Note regarding evaluation of this manuscript:** Manuscripts authored by scientists associated with Duke University, The University of North Carolina at Chapel Hill, Duke-NUS, and the Sanford-Burnham Medical Research Institute are handled not by members of the editorial board but rather by the science editors, who consult with selected external editors and reviewers.

**Conflict of interest:** Bruce R. Blazar, John C. Byrd, Jason A. Dubovsky, and Ryan Flynn have filed for intellectual patent rights on aspects of the current research. Laurence Elias is an employee of Pharmacyclis Inc., the company that owns ibrutinib.

**Submitted:** January 22, 2014; **Accepted:** August 21, 2014.

**Reference information:** *J Clin Invest*. 2014;124(11):4867–4876. doi:10.1172/JCI75328.

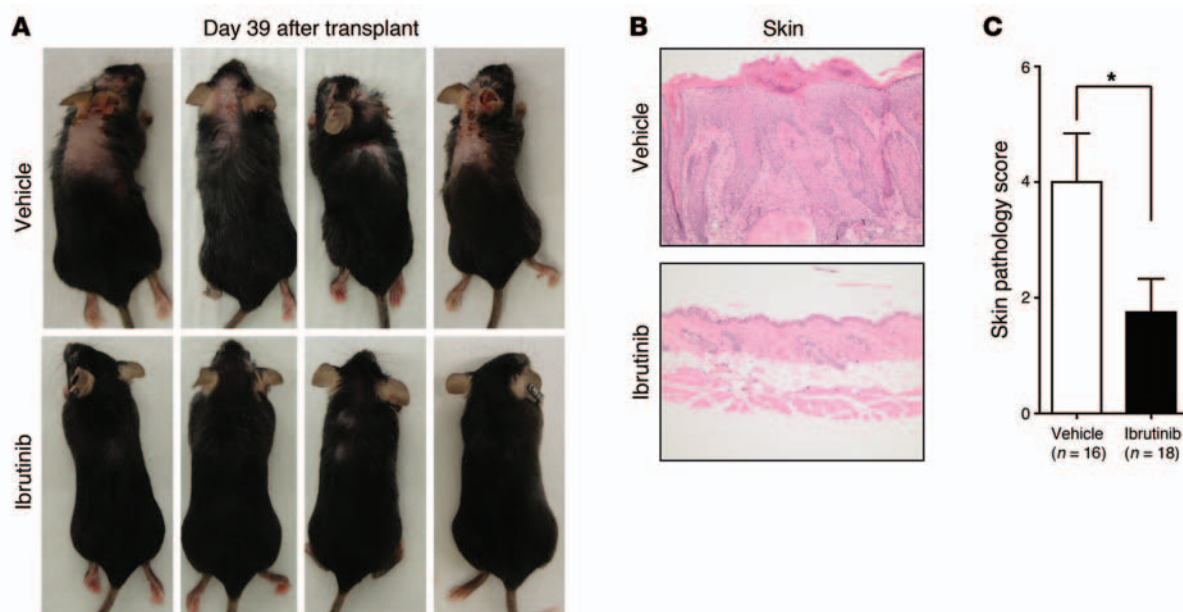


**Figure 1. Scleroderma and skin manifestations of cGVHD are alleviated by ibrutinib therapy.** At day 25 after HSCT, a total of 18 mice (from 2 independent experiments) were randomly assigned to ibrutinib (25 mg/kg/d), 18 to vehicle, and 11 to cyclosporine (10 mg/kg/d). Sclerodermatous lesions, hair loss, hunched posture, and gaunt appearance are characteristic visual indicators of cGVHD in this model. **(A)** Representative visual analysis of 4 randomly selected mice at day 39 after HSCT. **(B)** H&E-stained skin preparations of sclerodermatous skin lesions showing levels of dermal fibrosis, epidermal hyperplasia, serocellular crusting, erosion, and lymphohistiocytic infiltration, consistent with cGVHD. Original magnification,  $\times 200$ . **(C)** Pathologic cGVHD involvement of the skin was independently assessed on a scale from 0 to 8 for each mouse. Cohort averages are displayed. \* $P < 0.05$ . Error bars indicate SEM.

vation of NF- $\kappa$ B, MAPK, and nuclear factor of activated T cells (NFAT) in lymphocytes, resulting in cellular activation, release of soluble effector molecules, and rapid proliferation (18). Antibody production by B cells hinges upon the function of BTK (17). Whereas Th1, Treg, and CD8<sup>+</sup> effector T cells have both ITK and resting lymphocyte kinase (RLK, aka TTX) to drive activation, epigenetic evolution of Th2 and Th17 cells conserves a singular dominant role for ITK (19–24). This TEC-kinase profile difference provides an avenue to selectively target T cell subsets potentially highly relevant to cGVHD. However, to date, the individual impact of BTK or ITK on the development of cGVHD is unknown.

Ibrutinib is a first-in-class irreversible inhibitor of BTK and ITK that blocks downstream immune receptor activation (25–27). Numerous in vitro and in vivo studies confirm the specific activity and clinical safety of ibrutinib for the treatment of specific TEC-kinase-dependent malignancies (28–31). Since ibrutinib can block the activation of B cells via BTK inhibition as well as specific T helper subsets that drive the development of cGVHD via ITK inhibition, we hypothesized that it may be ideally suited to the treatment of cGVHD.

To study the multifaceted effects of this inhibitor in vivo and interrogate the activity of both T and B cells in the development of multiorgan systemic cGVHD, we used 2 complementary murine allogeneic HSCT models representing sclerodermatous and non-sclerodermatous cGVHD manifestations. Here, we show that ibrutinib treatment ameliorates the progression of cGVHD in the LP/J→C57BL/6 T cell-dependent murine model of sclerodermatous cGVHD, reducing skin lesions, hair loss, and lymphohistiocytic infiltration (32). Therapeutic administration of ibrutinib also proved effective at combating cGVHD in the C57BL/6→B10.BR

model, which develops bronchiolar obliterans (BO) syndrome and multiorgan cGVHD without skin involvement (7, 33). In this model, ibrutinib blocked germinal center (GC) formation and Ig deposition, reduced tissue fibrosis, and reversed BO-associated pulmonary dysfunction. Genetic studies confirmed that ITK and BTK are independently critical for the development of cGVHD. These data strongly support the clinical investigation of ibrutinib as a novel therapeutic strategy for the treatment of cGVHD.

## Results

**Therapeutic administration of ibrutinib limits the development of sclerodermatous lesions in a murine cGVHD model.** To assess the efficacy of ibrutinib as a therapeutic intervention for cGVHD, we used the LP/J→C57BL/6 model of sclerodermatous cGVHD, which develops dermal lesions characterized by hair loss, redness, flaking, scabbing, hunched posture, and thickened skin (32). In this murine model, symptoms become apparent between days 20 and 25 and peak between days 37 and 47 after HSCT. Ibrutinib or vehicle treatment was initiated in randomized cohorts at day 25, after the initial clinical signs of cGVHD (weight loss, hair loss, skin redness/flaking, hunched posture, or immobility) were visible in the majority (72%) of mice. Upon inspection at day 39 (14 days after starting therapy), ibrutinib-treated mice clearly lacked the sclerodermatous lesions, hair loss, hunched posture, and scabbing that were observed in both the vehicle and cyclosporine treatment groups (Figure 1A). The development of cGVHD in this model was not effectively constrained by 10 mg/kg/d cyclosporine therapy that is T cell immune suppressive (Supplemental Figure 1; supplemental material available online with this article; doi:10.1172/JCI75328DS1). Histology of representative skin lesions obtained

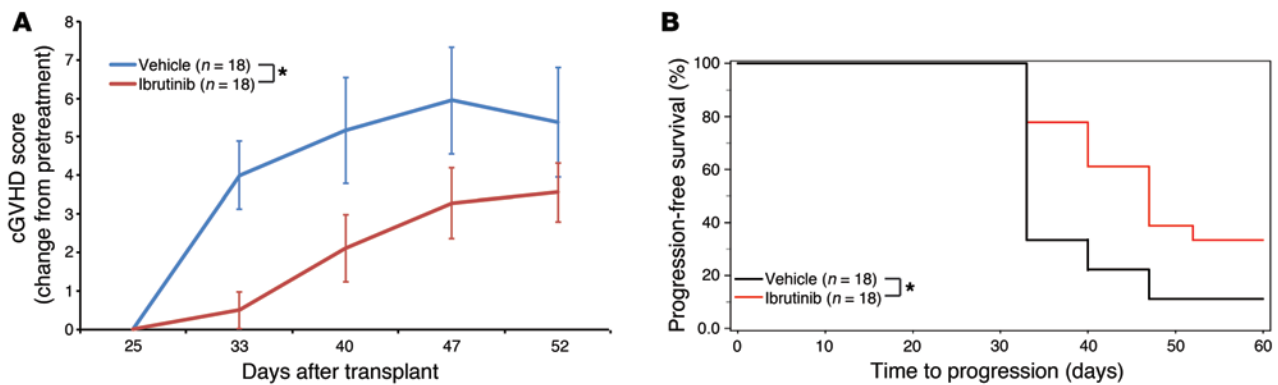


**Figure 2. Ibrutinib inhibits autoimmune manifestations of cGVHD.** (A) Weekly blinded analysis of cGVHD external metrics including weight, posture, vitality, mobility, coat, and skin in all mice from 2 independent experiments (18 vehicle and 18 ibrutinib) (Supplemental Table 1). All cGVHD scores were corrected for individual scores at the beginning of treatment (day 25). Error bars indicate SEM. \* $P < 0.01$ . (B) Kaplan-Meier plot of cGVHD progression-free survival. Data are derived from 2 independent experiments. Progression is defined as a greater than 2-point increase in day 25 cGVHD score (Supplemental Table 1) \* $P < 0.01$ .

at day 60 from vehicle- or cyclosporine-treated mice confirmed dermal fibrosis, epidermal hyperplasia, serocellular crusting, erosion, and lymphohistiocytic infiltration, which were not observed in skin samples from the ibrutinib-treated group (Figure 1, B and C, and Supplemental Figures 2 and 3).

*Ibrutinib improves sclerodermatous cGVHD progression-free survival and diminishes clinical and histopathological evidence of cGVHD.* To define cGVHD severity and progression in the LP/J→C57BL/6 model, we used a scoring system that quantitatively grades cGVHD metrics including the following: body weight, posture, mobility, hair loss, skin lesions, and vitality on a scale from 0 to 19 by a consistent and trained unbiased observer in a coded (blinded) manner (Supplemental Table 1 and ref. 34). Overall, 72% of mice (34 of 47) had active cGVHD on day 25, and the randomly assigned cohorts were very similar in initial (day 25) cGVHD score (ibrutinib = 1.5, vehicle = 1, cyclosporine = 2.9 of a possible 19). Using these metrics, we found that mice treated with ibrutinib significantly reduced the overall intensity of cGVHD compared with vehicle treatment ( $P = 0.0184$ ) (Figure 2A, Supplemental Table 1, and Supplemental Figure 4). Chronic GVHD progression in this model is defined as a greater than 2-point increase in cGVHD score from the initiation of therapy (Supplemental Table 1). Data derived from 2 independent experiments show that ibrutinib significantly extended median time to cGVHD progression by 14 days; moreover, 33% (6 of 18) of ibrutinib-treated mice remained progression free compared with 12% (2 of 18) receiving vehicle ( $P < 0.02$ ) (Figure 2B and Supplemental Figure 5). During the study period, we observed 100% survival in the ibrutinib cohort compared with 82% and 88% survival for cyclosporine and vehicle groups, respectively, which was not significant (Supplemental Figure 6). Weekly evaluation of mouse body weights revealed little variation between groups (Supplemental Figure 7).

In addition to the externally measurable cGVHD metrics, we demonstrated that the LP/J→C57BL/6 model consistently develops pulmonary and renal cGVHD among other cGVHD pathologies that are infrequently observed. Evaluation of H&E-stained sections revealed that, compared with vehicle controls, ibrutinib therapy reduced cGVHD-related aggregation of lymphocytes,

plasma cells, and histiocytes surrounding bronchioles and small caliber vessels throughout the pulmonary parenchyma and within the renal interstitium. Immunohistochemistry revealed B220<sup>+</sup> B cell and CD3<sup>+</sup> T cell pulmonary infiltration in addition to CD3<sup>+</sup> T cell renal infiltration in both the vehicle and cyclosporine groups, which was not observed in ibrutinib treatment groups (Figure 3A and Supplemental Figure 8). Coded pathologic analysis confirmed that ibrutinib improved systemic cGVHD in this model ( $P = 0.0099$  for lung and  $P = 0.0124$  for kidney) (Figure 3, B and C, and Supplemental Figures 9 and 10).

*Maximum ibrutinib therapeutic benefit in sclerodermatous cGVHD requires prolonged administration.* To understand the sustained therapeutic benefits of ibrutinib and the potential consequences of drug withdrawal, we conducted an additional long-term therapeutic experiment (Figure 3D). Once again, ibrutinib significantly limited cGVHD progression as compared with vehicle control ( $P = 0.0019$ ). We also found that withdrawal of therapy at day 60 permitted clinical breakthrough cGVHD in a single mouse (1 of 6); however, this was not statistically significant. A similar trend was observed by external cGVHD scoring (Supplemental Figure 11). Analysis of internal cGVHD pathology within the pulmonary and renal tissues on day 75 suggested that continuous long-term ibrutinib was more effective at controlling cGVHD; notably, internal pathology of the lung and kidney was not curtailed in BM-only recipients, indicating that certain cGVHD internal pathology in this model persists despite the elimination of T cells from the graft similar to what is observed in human allo-HSCT recipients (Supplemental Figure 12, A and B). Prophylactic ibrutinib treatment initiated pre-HSCT at day -2 and concluded at day 25 did not yield a significant improvement in cGVHD progression (Supplemental Figure 13), suggesting that ibrutinib will be most effective when T and B cell responses are more fully developed.

*Therapeutic administration of ibrutinib ameliorates pulmonary fibrosis and the development of BO.* cGVHD is characterized by a wide variety of autoimmune manifestations that are incompletely recapitulated by any single in vivo animal model. Recently published consensus criterion from the NIH considers BO the only pathognomonic manifestation of lung cGVHD (35). The C57BL/6→B10.BR



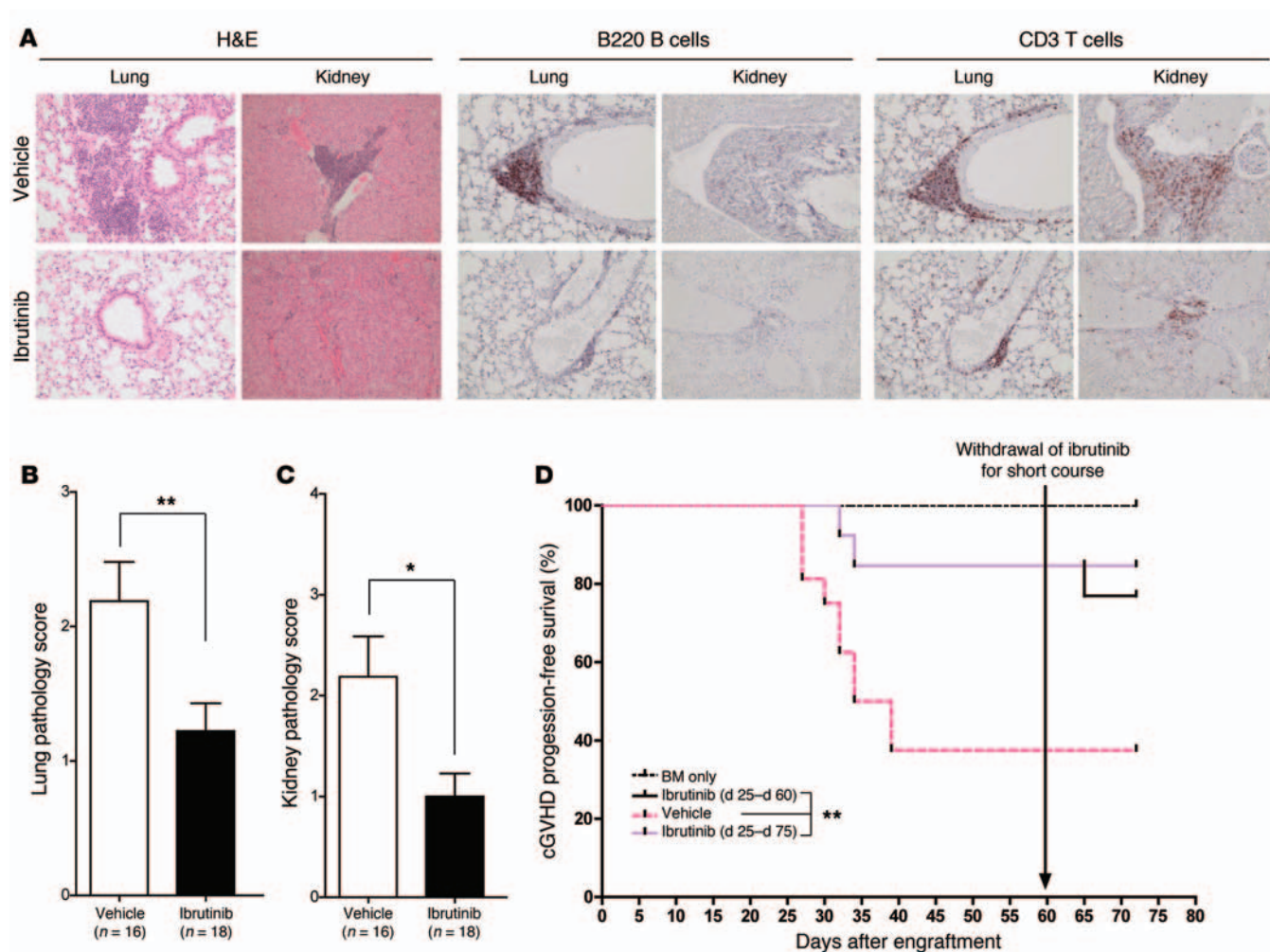


**Figure 3. Ibrutinib therapy prevents autoimmune injury in a T cell-dependent model of cGVHD.** (A) Representative images from H&E-, B220-, or CD3-stained lung and kidney tissues from mice sacrificed at day 125 after HSCT from 6 mice/group. Images were taken by a trained veterinary pathologist who was blinded to animal cohorts. Original magnification,  $\times 200$ . (B) Blinded pathologic analysis of H&E-stained lung tissues obtained from cGVHD cohorts (18 vehicle and 18 ibrutinib). Lymphohistiocytic infiltration was graded on a 0 to 4 scale for each animal. (C) Blinded pathologic analysis of H&E-stained kidney tissues obtained from cGVHD cohorts. Portal hepatitis and vasculitis were graded on a 0 to 4 scale for each animal.  $*P < 0.05$ ;  $**P < 0.01$ . (D) Kaplan-Meier plot of cGVHD progression-free survival in an independent experiment aimed to determine sustained benefits from continued ibrutinib therapy. During the course of the experiment, ibrutinib was withdrawn on day 60 from animals in the ibrutinib (day 25 to day 60) cohort.  $**P < 0.001$ .

model develops multiorgan system disease including BO starting at day 28 after HSCT. Therapeutic administration of ibrutinib beginning at day 28 and continuing indefinitely curtailed the development of BO in vivo as measured by pulmonary resistance ( $P = 0.0090$ ), elastance ( $P = 0.0019$ ), and compliance ( $P = 0.0071$ ) (Figure 4, A–C). Masson trichrome staining of inflated pulmonary tissues from 4 mice derived from 3 experiments revealed less peribroncheolar collagen fibrosis among ibrutinib-treated animals (Figure 4D) and a significant reduction in pulmonary fibrosis ( $P < 0.0001$ ) (Figure 4E). We observed 100% survival in the ibrutinib cohort versus 95% in the vehicle group (Supplemental Figure 14). Weekly evaluation of mouse body weight revealed little variation between groups (Supplemental Figure 15). To examine the sustained benefit of ibrutinib therapy, we conducted a separate set of experiments in which mice were withdrawn from ibrutinib on day 56 after transplant. Pulmonary function tests (PFTs) at day 60 and day 90 revealed that short-term ibrutinib therapy caused an eventual loss of benefit, supporting the need for continued thera-

py (Supplemental Figure 16). Day -2 to day 28 prophylactic administration of ibrutinib in this model also did not effectively combat cGVHD or BO (data not shown). Overall, these data indicate that ibrutinib therapy reduces the underlying fibrotic pathogenesis of BO in the C57BL/6 $\rightarrow$ B10.BR cGVHD model.

**Ibrutinib limits in vivo GC reactions and Ig deposition in pulmonary tissues.** Ibrutinib's ability to block B cell receptor-induced (BCR-induced) activation of BTK is well defined; however, it remains unclear whether GC reactions are effectively inhibited. To study this, we utilized the C57BL/6 $\rightarrow$ B10.BR mouse model in which robust GC reactions sustain pathogenic B lymphocytes and lead to Ig deposition within the liver and lungs and the development of BO. Peanut agglutinin staining revealed GC reactions within the spleen, and ibrutinib therapy reduced the overall size, cellularity, and number of GC reactions compared with those of vehicle-treated mice with active cGVHD ( $P < 0.001$ ) (Figure 5, A and B). On day 60 after HSCT, isolated splenocytes from chimeras were analyzed by flow cytometry for CD19 $^{+}$ GL7 $^{+}$ CD38 $^{lo}$  GC

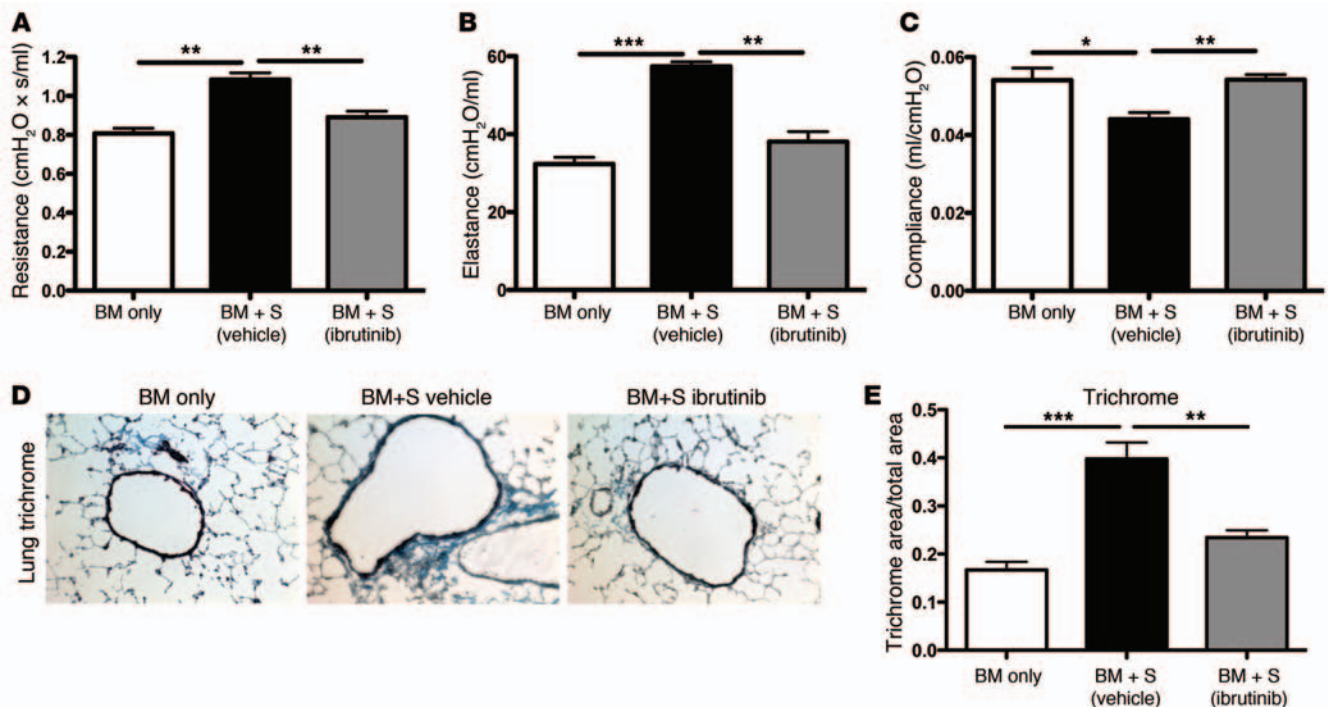


**Figure 4. Collagen deposition and pulmonary function are improved in a murine model of bronchiolitis obliterans.** (A–C) PFTs were performed at day 60 after transplant on anesthetized animals. Animals ( $n = 4/\text{group}$ ) were artificially ventilated and (A) resistance, (B) elastance, and (C) compliance were measured as parameters of distress in lung function in animals receiving  $5 \times 10^6$  splenocytes (S) in addition to BM. Error bars indicate SEM. (D and E) Collagen deposition within pulmonary tissues was determined with a Masson trichrome staining kit; blue indicates collagen deposition. (D) Representative images of collagen deposition observed in each treatment cohort ( $n = 8$ ). Blue staining represents Masson trichrome–stained collagen. Original magnification,  $\times 200$ . (E) Quantification of collagen deposition ( $n = 8$ ) as a ratio of blue area to total area of tissue was performed with the analysis tool in Photoshop CS3. Representative data from 3 independent experiments. \* $P < 0.05$ ; \*\* $P < 0.01$ ; \*\*\* $P < 0.001$ .

B cells. Ibrutinib significantly inhibited the cGVHD-induced formation of GCs within the spleen ( $P = 0.0222$ ) to numbers comparable to those in the no cGVHD, BM only control (Figure 5C).

The functional product of alloreactive GC B cells is secreted Ig, which deposits within healthy tissues. In the C57BL/6→B10.BR cGVHD model, BO is inextricably related to the deposition of soluble Ig within pulmonary tissues and the fibrotic cascade that this initiates. By blocking B cell reactivity, ibrutinib limited pulmonary deposition of Ig as quantified at day 60 after HSCT using immunofluorescent microscopy (Figure 5D). Quantification of the immunofluorescent signal revealed elimination of pulmonary Ig deposition after therapeutic ibrutinib treatment ( $P < 0.001$ ) (Figure 5E). Together, these data confirm that a clinically relevant downstream effect of ibrutinib therapy in the setting of cGVHD is the blockade of Ig deposition within healthy tissues.

*Genetic ablation of BTK or ITK activity in allogeneic donor cell engraftment confirms that both TEC kinases are required for the development of cGVHD.* The XID mouse in which the kinase activity of BTK is genetically abrogated and the *Itk*<sup>−/−</sup> mouse have been fully characterized on the C57BL/6 genetic background (36, 37). Given ibrutinib's ability to inhibit both ITK and BTK, we sought to examine the relative independent contributions of ITK and BTK to the development of cGVHD. We therefore examined pulmonary function at day 60 after HSCT, as this represents a primary functional measurement of cGVHD-induced lung injury and fibrosis in the C57BL/6→B10.BR model.

Chronic GVHD sustaining T cells in this model originate from mature lymphocytes in the donor cell graft. To recapitulate the effect of ITK inhibition within these cGVHD-causative T lymphocytes, we administered *Itk*<sup>−/−</sup> splenic T cells along with BM from WT mice to allogeneic recipients. Day 60 PFTs including resistance, elastance, and compliance were uniformly and significantly ( $P = 0.0014$ ;  $P = 0.0028$ ;  $P = 0.0003$ ) reduced in mice receiving *Itk*<sup>−/−</sup> versus WT splenic T cells and comparable to non-cGVHD, BM-only controls (Figure 6). These data reveal that T cell ITK activity is necessary for the development of cGVHD.

Data from both models implicates hyperreactive BTK in B cells isolated from both cGVHD models (Supplemental Figure 17). To genetically confirm the role of BTK signaling in cGVHD, we infused XID BM along with WT splenic T cells to mimic BTK inhibition. PFTs conducted at day 60 after HSCT revealed that BTK activity was essential to the development of BO (Figure 7). Pulmonary resistance, elastance, and compliance were significantly reduced in recipients of WT T cells and XID versus WT BM ( $P = 0.0025$ ;  $P = 0.0025$ ;  $P = 0.0496$ ) and comparable to XID or WT BM-only controls.

*Ibrutinib blocks T and B cell activation in samples obtained from patients with active cGVHD.* Our data confirm that BTK and ITK are critical to the development of cGVHD and that ibrutinib works to alleviate the symptoms associated with severe cGVHD in murine models. To confirm that this effect is not restricted to mouse models, we tested the effects of ibrutinib on CD4 T and



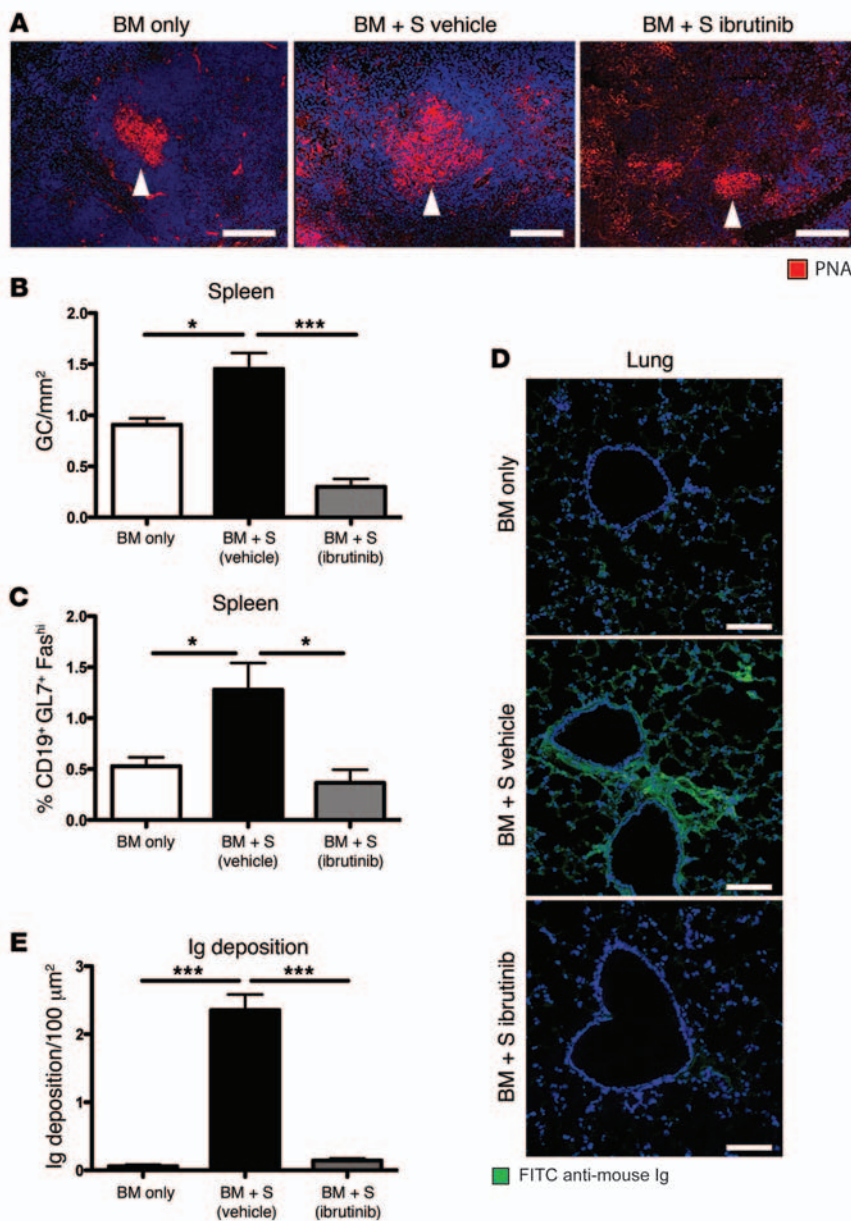


**Figure 5. GC reactions and pulmonary immunoglobulin deposition are reduced with administration of ibrutinib.** (A) GCs were imaged by staining 6- $\mu$ m spleen sections with PNA conjugated to rhodamine (red) and DAPI (blue). (B) GC area (GC/mm<sup>2</sup>) was calculated from PNA-stained immunofluorescent images for each animal. The average area for each cohort is displayed. Error bars indicate SEM. (C) Splenocytes were purified from transplanted mice on day 60, and frequency of GC B cells was quantified. (D) 6- $\mu$ m lung sections from day 60 transplanted mice were stained with anti-mouse Ig conjugated to FITC (green) and DAPI (blue) and (E) quantified with Adobe Photoshop CS3. Representative data from 3 independent experiments. \* $P < 0.05$ ; \*\*\* $P < 0.001$ . All measurements were conducted on day 60 after HSCT. Scale bars: 100  $\mu$ m.

B cells obtained from patients with active and persistent cGVHD. Data revealed that after pretreatment with 1  $\mu$ M ibrutinib, CD4<sup>+</sup> T cells from these patients demonstrated lower surface expression of CD69 after ex vivo T cell receptor (TCR) stimulation using anti-CD3 ( $P = 0.033$ ) (Figure 8A). Moreover, purified B cells that were pretreated with 1  $\mu$ M ibrutinib showed lower levels of pBTK-Y223, pPLC $\gamma$ 2-Y1217, and pERK1/2 by immunoblot analysis (Figure 8B). These data confirm that ibrutinib can curtail immune receptor activation of human B and T cells in the setting of active cGVHD.

## Discussion

Chronic GVHD develops from coordinated effects of both B and T cells, and multiple key functions of these cells are driven by TEC family kinases. Here, we show that neither XID BM nor *Itk*<sup>-/-</sup> donor T cells facilitate the development of systemic cGVHD in mice, identifying the importance of the TEC kinases BTK and ITK in cGVHD and identifying these 2 enzymes as therapeutic targets

in this disease. Therefore, because of its ability to simultaneously target BTK and ITK, ibrutinib holds specific promise for the treatment of cGVHD. Our studies utilize 2 distinct but complementary, validated murine models of cGVHD: one that has dominant sclerodermatous features and the other with a nonsclerodermatous, multiorgan system fibrotic disease with BO (32, 33). Our results indicate that ibrutinib targets B and T cell-driven GC responses and is remarkably effective in treating cGVHD. In the sclerodermatous model, animals receiving therapeutic ibrutinib were often indistinguishable from their healthy counterparts, and in the nonsclerodermatous cGVHD model, no cGVHD manifestations were evident even at the end of the observation period. Moreover, GC reaction size, cellularity, and number were lower in mice receiving ibrutinib, correlating to a partial but significant resolution of cGVHD symptoms. These data are consistent with pre-clinical data in which GC reactions are key to cGVHD pathogenesis; for instance, clinical responses to rituximab (anti-CD20 mAb) have been observed, implicating B cells as etiopathogenic in human cGVHD (38–40). Finally, we confirmed that our observation could be applied to human therapy by testing ibrutinib's capacity to block the molecular activation of T cells and B cells directly obtained from patients with active ongoing cGVHD.

Results from our genetic ablation models reveal that BM-derived B cells depend upon BTK for GC formation. Similarly, *Itk*<sup>-/-</sup> splenocytes are unable to cause cGVHD, suggesting that ITK is critical for T cell support of the fibrotic cascade. While XID and *Itk*<sup>-/-</sup> mice are useful in exploring the mechanisms responsible for cGVHD generation, there are caveats. For instance, TEC kinase has been shown to compensate for the lack of BTK in the XID mouse model, and complete genetic ablation of ITK blunts thymic maturation of functionally mature T lymphocytes (18, 41, 42). As a result, we can conclude that ITK and BTK are necessary components for the development of cGVHD; however, we cannot

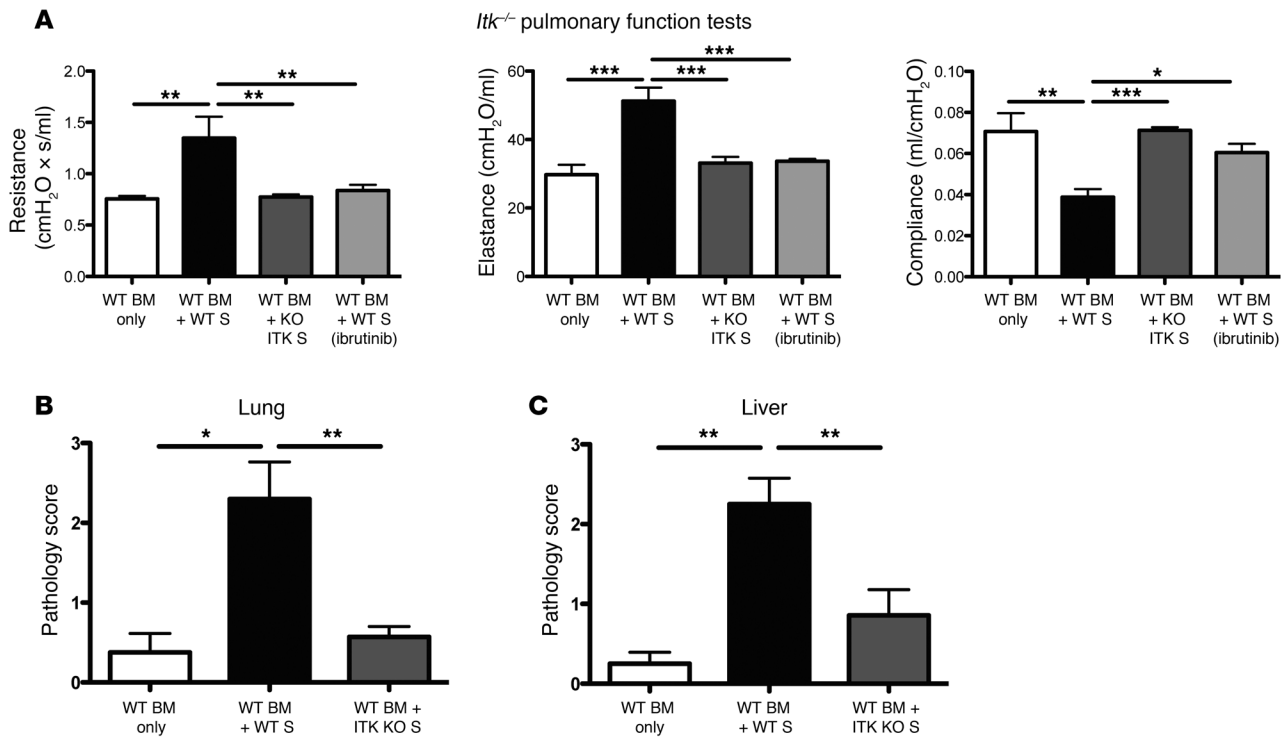


**Figure 6. Development of BO is dependent on ITK expression in donor mature T cells. (A)** Day 60 PFTs from mice transplanted with WT BM and low numbers of either WT T cells or ITK-deficient T cells. **(B)** Pathologic scores in lung and **(C)** liver of day 60 transplanted mice.  $n = 5$  mice/group in 2 independent experiments. \* $P < 0.05$ ; \*\* $P < 0.01$ ; \*\*\* $P < 0.001$ .

conclude that ibrutinib's therapeutic efficacy is solely driven by inhibition of these 2 TEC kinases.

In the cGVHD model that has BO as an important feature, fibrosis occurs by day 28 after HSCT. Intriguingly, ibrutinib treatment beginning on day 28 after HSCT in mice with established cGVHD resulted in resolution of fibrosis, suggesting that treatment in the early phase of cGVHD can permit tissue repair and further suggesting that ongoing antibody deposition in cGVHD target organs may be required for a persistent fibrogenic process. Notably, for patients with debilitating cGVHD from fibrosis, therapies include supportive care, high-dose steroids, rapamycin, mycophenolate, imatinib, extracorporeal photopheresis, IL-2, and lung transplant, all with incomplete efficacy and potentially serious complications (43–55). Although conclusions from rodent cGVHD must be validated in patients, our studies collectively indicate that a wide spectrum of cGVHD patients may benefit from ibrutinib therapy.

To examine the importance of sustained therapy, we conducted studies using both cGVHD models in which mice were withdrawn from ibrutinib therapy around day 60 after HSCT. In general, we observed a loss of efficacy with removal of the drug; however, not all metrics were statistically significant. These data are consistent with our molecular understanding, which would imply that pathogenic T cells and B cells are restrained by the inhibitor but not actively depleted. Overall, these data would direct caution in the clinical setting when attempting to taper such an inhibitor after relatively short time periods.

To study prophylactic efficacy, we initiated ibrutinib treatment 2 days prior to HSCT and continued until we begin to observe

cGVHD (approximately 28 days). Although posttransplant administration of ibrutinib effectively controlled cGVHD, we found that prophylactic treatment was ineffective under these conditions. The ideal time frame for ibrutinib administration may coincide with the establishment of robust T cell-driven GC reactions that may take up to 1 month; prophylactic treatment alone may be ineffective for this reason. Furthermore, unlike rituximab, ibrutinib does not directly kill B cells; instead, it prevents downstream BCR activation, arresting cells in an unstimulated state. This effect can be lost after withdrawal of ibrutinib. Together, our data indicate that ibrutinib is likely to be better for cGVHD therapy as opposed to prophylaxis, should preclinical studies translate into the clinic.

Our studies focus on ibrutinib's effect on cGVHD; however, the effects on infectious complications and leukemic relapse remain unknown. Recent mouse and human studies indicate that ibrutinib improves immune competence with regard to infectious complications; however, this has yet to be tested in the HSCT setting (27, 30). Ibrutinib also has direct antileukemic effects in both B cell-derived tumors and acute myeloid leukemia (AML), supporting the notion that it may directly aid in relapse prevention (56, 57).

Overall, our complementary *in vivo* models demonstrate a clear therapeutic benefit derived from therapeutic administration of ibrutinib to reduce the prolonged autoimmune effects of cGVHD. In addition, our *ex vivo* human data suggest that these conclusions likely extend to the setting of human cGVHD. These data support the future study of this promising therapeutic agent in cGVHD as well as the exploration of novel strategies that target specific TEC kinases in the setting of allo-HSCT.



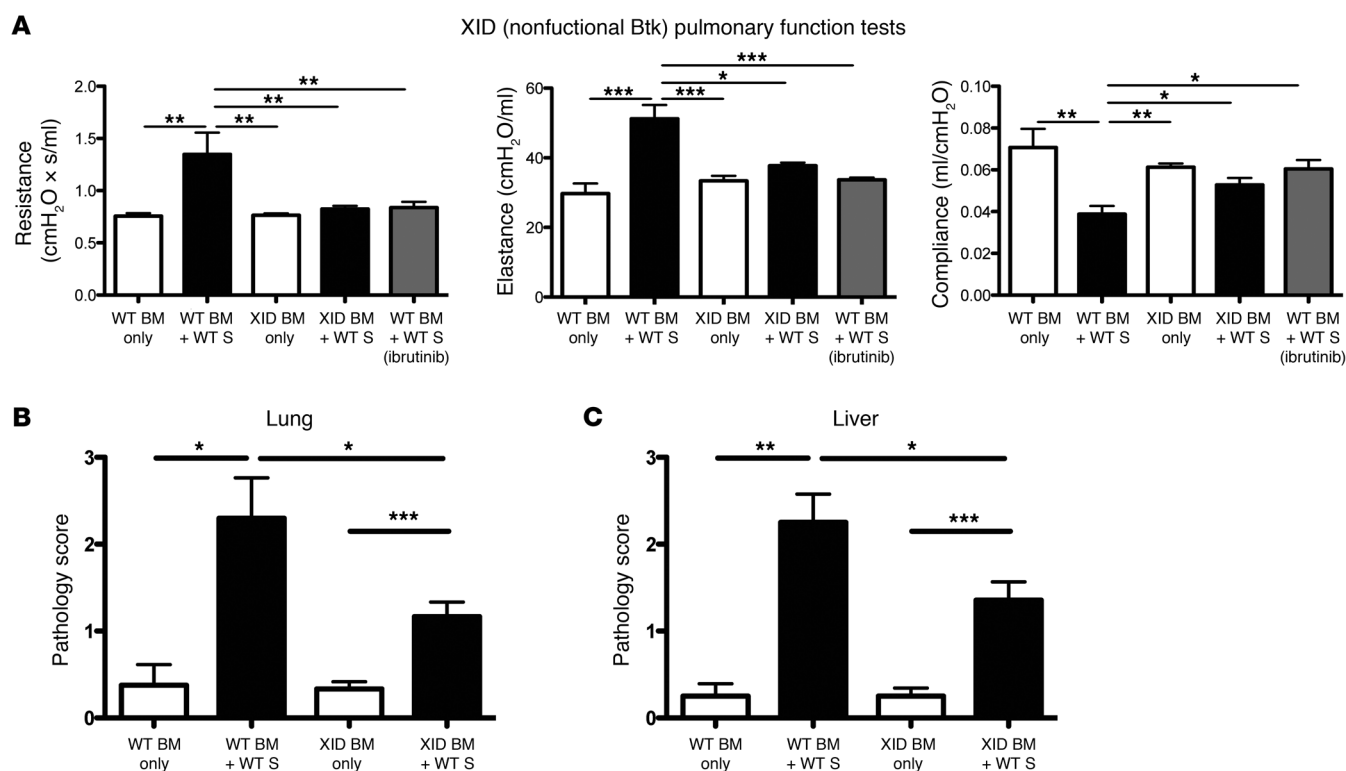


**Figure 7. Expression of BTK in donor-derived B cells is necessary for the development of BO.** (A) Day 60 PFTs from mice transplanted with low levels of WT T cells and either WT or XID (kinase inactive BTK) BM. (B) Pathologic scores in lung and (C) liver of day 60 transplanted mice.  $n = 5$  mice/group from 2 independent experiments. \* $P < 0.05$ ; \*\* $P < 0.01$ ; \*\*\* $P < 0.001$ .

## Methods

**Mice.** C57BL/6 (H2<sup>b</sup>) mice were purchased from the National Cancer Institute or from The Jackson Laboratory. LP/J and B10.BR (H2<sup>b</sup>) mice were purchased from The Jackson Laboratory. The C57BL/6 XID mouse, in which a specific mutation abrogates BTK kinase activity, was obtained from The Jackson Laboratory. The C57BL/6 *Itk*<sup>-/-</sup> mouse was a gift from Leslie Berg (University of Massachusetts, Boston, Massachusetts, USA) (58). Both strains are maintained on the defined C57BL/6 genetic background (36, 37). All mice were housed in a pathogen-free facility at The Ohio State University or The University of Minnesota.

**Therapeutic HSCT models.** The C57BL/6→B10.BR model has been described previously (7). In brief, B10.BR recipients conditioned with 120 mg/kg/d i.p. cyclophosphamide (Cy) on days -3 and -2 and 8.3 Gy TBI (using a <sup>137</sup>Cesium irradiator) on day -1 were engrafted with  $1 \times 10^7$  Thy1.2-depleted C57BL/6 derived BM cells with (or without)  $1 \times 10^6$  allogeneic splenocytes.

Experiments with the LP/J→C57BL/6 model were conducted using methods similar to those previously described (32). Briefly, C57BL/6 recipients were conditioned with 8.5 Gy x-ray TBI on day 0 and were provided  $1 \times 10^7$  LP/J-derived BM cells and  $2 \times 10^6$  spleno-

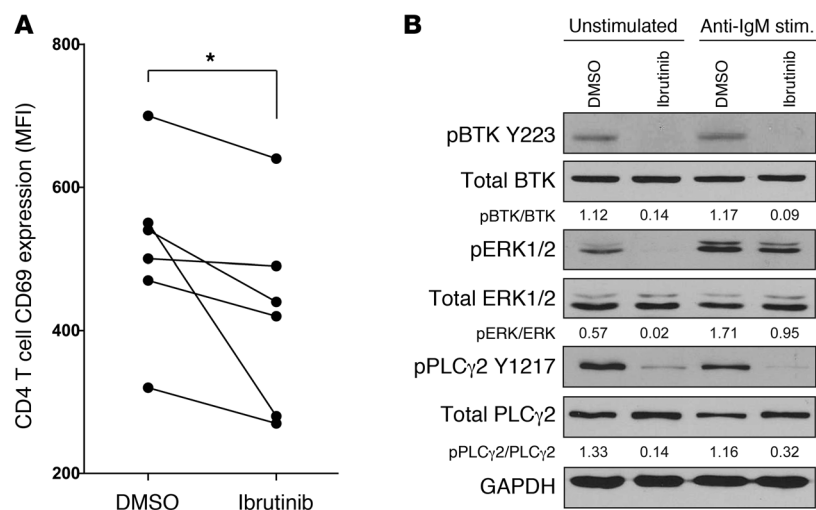


**Figure 8. Ibrutinib limits activation of T cells and B cells from patients with active cGVHD.** (A) Primary CD4<sup>+</sup> T cells were isolated from patients with active cGVHD, pretreated with 1  $\mu$ M ibrutinib (or DMSO), and stimulated using anti-CD3 for 6 hours. Graph shows the mean fluorescence intensity (MFI) for CD69 among CD4<sup>+</sup> T cells for each patient. \* $P < 0.05$ . (B) B cells isolated from patients with cGVHD were pretreated with 1  $\mu$ M ibrutinib and stimulated with anti-IgM for 45 minutes. Immunoblot analysis of BTK, ERK, and PLCγ2 was conducted. The densitometric quantification of activated proteins relative to total proteins is provided. Data are representative of 3 experiments on 3 separate patients.

cytes by tail-vein injection. Mice surviving to day 25 begin to show clinical and pathological changes consistent with systemic cGVHD, frequently involving the skin, lung, and kidneys and infrequently involving hepatic or salivary gland lymphohistiocytic infiltration, conjunctivitis, anterior uveitis, esophagitis, and corneal ulcers. In our hands, this specific splenocyte and irradiation dose produces a cGVHD phenotype, devoid of the classic gastrointestinal lesions, splenic atrophy, or diarrhea associated with acute GVHD (aGVHD). The development of cGVHD was measured in coded fashion using a modified version of the scoring system originally described by Cooke et al. (Supplemental Table 1 and ref. 34).

Therapeutic administration of ibrutinib (provided by L. Elias) via drinking water was conducted as previously described (27). Mice received a dose of 15 mg/kg/d ibrutinib in 0.4% methylcellulose by i.p. injection starting at day 28 after transplant for the C57BL/6→B10.BR model or 25 mg/kg/d via drinking water starting at day 25 after transplant for the LP/J→C57BL/6 model. Drinking water administration daily dose was calculated previously (Supplemental Table 2). In the latter strain combination, a cohort of mice was given cyclosporine A administered i.p. in 0.2% CMC at 10 mg/kg/d starting at day 25 for 2 weeks followed by thrice weekly as previously described (59). Unless otherwise stated, ibrutinib was administered until the end of the study.

For both cGVHD models, the BTK pathway was found to be constitutively activated, similar to what has been identified in human cGVHD (Supplemental Figure 17).

**PFTs.** PFTs were performed on anesthetized mice using whole-body plethysmography with the Flexivent system (SCIREQ) as previously described (7, 33).

**GC detection.** GC detection was conducted with 6- $\mu$ m spleen cryosections stained using rhodamine peanut agglutinin as previously described (7).

**Masson trichrome staining.** Cryosections (6  $\mu$ m) were fixed for 5 minutes in acetone and stained with H&E and with the Masson Trichrome Staining Kit (Sigma-Aldrich) for detection of collagen deposition. Collagen deposition was quantified on trichrome-stained sections as a ratio of area of blue staining to area of total staining using the Adobe Photoshop CS3 analysis tool.

**Histopathological scoring.** Coded pathologic analysis of H&E-stained sections was performed by A. Panoskaltsis-Mortari or B.K. Harrington in an unbiased manner with scores ranging from 0 to 4

(60). For pulmonary tissues, scores indicate the number of lymphoplasmacytic and histiocytic cellular cuffs infiltrating the surrounding airways or vasculature and the number of infiltrating aggregates. For renal H&E-stained sections, both perivascular lymphoplasmacytic infiltration and intratubular protein were quantified. For additional details, see Supplemental Methods.

**Immunoblot analysis.** Experiments were conducted using conventional methodology previously described (61). Blotting was conducted using pBTK-Y223-, BTK-, pPLC $\gamma$ 2-Y1217-, PLC $\gamma$ 2-, pERK1/2-, ERK-, and GAPDH-specific antibodies (Cell Signaling Technologies).

**Statistics.** A 2-tailed Student's *t* test was used for normal data at equal variance. Significance was defined as *P* < 0.05. For cGVHD scoring in the LP/J→C57BL/6 model, a linear mixed effects model was applied to assess the trends in cGVHD scores from days 33 to 52, using the measurement at day 25 as a covariate to account for differences in the initial measurement between treatments. Chronic GVHD progression in the LP/J→C57BL/6 model was prospectively defined as a greater than 2-point increase in cGVHD score from the initiation of therapy (Supplemental Table 1).

**Study approval.** All animal studies were approved by the institutional animal care committees at The Ohio State University and the University of Minnesota.

## Acknowledgments

The authors gratefully acknowledge Leslie J. Berg for providing critical reagents as well as Jessica MacMurray for experimental assistance. This work was supported by grants from the NIH (P01 AI056299, P01 CA142106, R01 HL56067, and R01 AI34495 to B.R. Blazar; T32 AI1007313 to R. Flynn). In addition, support was provided by National Cancer Institute grants (P01 CA095426, K12 CA133250-05, and P50 CA140158 to J.C. Byrd; T32 CA009338-33-03 to J.A. Dubovsky), as well as grants from the American Cancer Society (125039-PF-13-246-01-LIB to J.A. Dubovsky), the Leukemia & Lymphoma Society, the American Society of Hematology, Mr. and Mrs. Michael Thomas, the Harry Mangurian Foundation, the D. Warren Brown Family Foundation, and the Jock and Bunny Adams Research and Education Endowment (to J.H. Antin).

Address correspondence to: Bruce R. Blazar, MMC 109, University of Minnesota, Minneapolis, Minnesota 55455, USA. Phone: 612.626.2734; E-mail: blaza001@umn.edu.

- Baird K, Pavletic SZ. Chronic graft versus host disease. *Curr Opin Hematol*. 2006;13(6):426–435.
- Lee SJ, Vogelsang G, Flowers ME. Chronic graft-versus-host disease. *Biol Blood Marrow Transplant*. 2003;9(4):215–233.
- Pidala J, et al. Patient-reported quality of life is associated with severity of chronic graft-versus-host disease as measured by NIH criteria: report on baseline data from the Chronic GVHD Consortium. *Blood*. 2011;117(17):4651–4657.
- Arai S, et al. Global and organ-specific chronic graft-versus-host disease severity according to the 2005 NIH Consensus Criteria. *Blood*. 2011;118(15):4242–4249.
- Holler E. Risk assessment in haematopoietic stem cell transplantation: GvHD prevention and treatment. *Best Pract Res Clin Haematol*. 2007;20(2):281–294.
- Coghill JM, Sarantopoulos S, Moran TP, Murphy WJ, Blazar BR, Serody JS. Effector CD4<sup>+</sup> T cells, the cytokines they generate, and GVHD: something old and something new. *Blood*. 2011;117(12):3268–3276.
- Srinivasan M, et al. Donor B-cell alloantibody deposition and germinal center formation are required for the development of murine chronic GVHD and bronchiolitis obliterans. *Blood*. 2012;119(6):1570–1580.
- Lim JY, et al. Fluctuations in pathogenic CD4<sup>+</sup> T-cell subsets in a murine sclerodermatous model of chronic graft-versus-host disease. *Immunol Invest*. 2014;43(1):41–53.
- Fujii H, et al. Biomarkers in newly diagnosed pediatric-extensive chronic graft-versus-host disease: a report from the Children's Oncology Group. *Blood*. 2008;111(6):3276–3285.
- Sarantopoulos S, et al. High levels of B-cell activating factor in patients with active chronic graft-versus-host disease. *Clin Cancer Res*. 2007;13(20):6107–6114.
- Sarantopoulos S, et al. Altered B-cell homeostasis and excess BAFF in human chronic graft-versus-host disease. *Blood*. 2009;113(16):3865–3874.
- She K, et al. Altered Toll-like receptor 9 responses in circulating B cells at the onset of extensive chronic graft-versus-host disease. *Biol Blood Marrow Transplant*. 2007;13(4):386–397.
- Carlson MJ, West ML, Coghill JM, Panoskaltsis-Mortari A, Blazar BR, Serody JS. In vitro-differentiated TH17 cells mediate lethal acute graft-versus-host disease with severe cutaneous

- and pulmonary pathologic manifestations. *Blood*. 2009;113(6):1365–1374.
14. Zhang Y, Hexner E, Frank D, Emerson SG. CD4<sup>+</sup> T cells generated de novo from donor hemopoietic stem cells mediate the evolution from acute to chronic graft-versus-host disease. *J Immunol*. 2007;179(5):3305–3314.
  15. Radojic V, et al. STAT3 signaling in CD4<sup>+</sup> T cells is critical for the pathogenesis of chronic sclerodermatous graft-versus-host disease in a murine model. *J Immunol*. 2010;184(2):764–774.
  16. Berg LJ, Finkelstein LD, Lucas JA, Schwartzberg PL. Tec family kinases in T lymphocyte development and function. *Annu Rev Immunol*. 2005;23:549–600.
  17. Satterthwaite AB, Witte ON. The role of Bruton's tyrosine kinase in B-cell development and function: a genetic perspective. *Immunol Rev*. 2000;175:120–127.
  18. Gomez-Rodriguez J, Kraus ZJ, Schwartzberg PL. Tec family kinases Itk and Rlk / Txk in T lymphocytes: cross-regulation of cytokine production and T-cell fates. *FEBS J*. 2011;278(12):1980–1989.
  19. Schaeffer EM, et al. Mutation of Tec family kinases alters T helper cell differentiation. *Nat Immunol*. 2001;2(12):1183–1188.
  20. Mueller C, August A. Attenuation of immunological symptoms of allergic asthma in mice lacking the tyrosine kinase ITK. *J Immunol*. 2003;170(10):5056–5063.
  21. Au-Yeung BB, Katzman SD, Fowell DJ. Cutting edge: Itk-dependent signals required for CD4<sup>+</sup> T cells to exert, but not gain, Th2 effector function. *J Immunol*. 2006;176(7):3895–3899.
  22. Sahu N, et al. Selective expression rather than specific function of Txk and Itk regulate Th1 and Th2 responses. *J Immunol*. 2008;181(9):6125–6131.
  23. Fowell DJ, et al. Impaired NFATc translocation and failure of Th2 development in Itk-deficient CD4<sup>+</sup> T cells. *Immunity*. 1999;11(4):399–409.
  24. Miller AT, Wilcox HM, Lai Z, Berg LJ. Signaling through Itk promotes T helper 2 differentiation via negative regulation of T-bet. *Immunity*. 2004;21(1):67–80.
  25. Chang BY, et al. The Bruton tyrosine kinase inhibitor PCI-32765 ameliorates autoimmune arthritis by inhibition of multiple effector cells. *Arthritis Res Ther*. 2011;13(4):R115.
  26. Herman SE, et al. Bruton tyrosine kinase represents a promising therapeutic target for treatment of chronic lymphocytic leukemia and is effectively targeted by PCI-32765. *Blood*. 2011;117(23):6287–6296.
  27. Dubovsky JA, et al. Ibrutinib is an irreversible molecular inhibitor of ITK driving a Th1 selective pressure in T-lymphocytes. *Blood*. 2013;122(15):2539–2549.
  28. Woyach JA, Johnson AJ, Byrd JC. The B-cell receptor signaling pathway as a therapeutic target in CLL. *Blood*. 2012;120(1):9.
  29. Honigberg LA, et al. The Bruton tyrosine kinase inhibitor PCI-32765 blocks B-cell activation and is efficacious in models of autoimmune disease and B-cell malignancy. *Proc Natl Acad Sci U S A*. 2010;107(29):13075–13080.
  30. Byrd JC, et al. Targeting BTK with ibrutinib in relapsed chronic lymphocytic leukemia. *N Engl J Med*. 2013;369(1):32–42.
  31. Wang ML, et al. Targeting BTK with ibrutinib in relapsed or refractory mantle-cell lymphoma. *N Engl J Med*. 2013;369(6):507–516.
  32. Hamilton BL, Parkman R. Acute and chronic graft-versus-host disease induced by minor histocompatibility antigens in mice. *Transplantation*. 1983;36(2):150–155.
  33. Panoskaltis-Mortari A, Tram KV, Price AP, Wendt CH, Blazar BR. A new murine model for bronchiolitis obliterans post-bone marrow transplant. *Am J Respir Crit Care Med*. 2007;176(7):713–723.
  34. Cooke KR, et al. An experimental model of idiopathic pneumonia syndrome after bone marrow transplantation: I. The roles of minor H antigens and endotoxin. *Blood*. 1996;88(8):3230–3239.
  35. Filipovich AH, et al. National Institutes of Health consensus development project on criteria for clinical trials in chronic graft-versus-host disease: I. Diagnosis and staging working group report. *Biol Blood Marrow Transplant*. 2005;11(12):945–956.
  36. Numata F, Hitoshi Y, Uehara S, Takatsu K. The xid mutation plays an important role in delayed development of murine acquired immunodeficiency syndrome. *Int Immunol*. 1997;9(1):139–146.
  37. Liu KQ, Bunnell SC, Gurniak CB, Berg LJ. T cell receptor-initiated calcium release is uncoupled from capacitative calcium entry in Itk-deficient T cells. *J Exp Med*. 1998;187(10):1721–1727.
  38. Kharfan-Dabaja MA, Cutler CS. Rituximab for prevention and treatment of graft-versus-host disease. *Int J Hematol*. 2011;93(5):578–585.
  39. Kharfan-Dabaja MA, Mhaskar AR, Djulbegovic B, Cutler C, Mohty M, Kumar A. Efficacy of rituximab in the setting of steroid-refractory chronic graft-versus-host disease: a systematic review and meta-analysis. *Biol Blood Marrow Transplant*. 2009;15(9):1005–1013.
  40. Teshima T, et al. Rituximab for the treatment of corticosteroid-refractory chronic graft-versus-host disease. *Int J Hematol*. 2009;90(2):253–260.
  41. Tomlinson MG, Kane LP, Su J, Kadlecak TA, Mollenauer MN, Weiss A. Expression and function of Tec, Itk, and Btk in lymphocytes: evidence for a unique role for Tec. *Mol Cell Biol*. 2004;24(6):2455–2466.
  42. Ellmeier W, et al. Severe B cell deficiency in mice lacking the tec kinase family members Tec and Btk. *J Exp Med*. 2000;192(11):1611–1624.
  43. Inamoto Y, Flowers ME. Treatment of chronic graft-versus-host disease in 2011. *Curr Opin Hematol*. 2011;18(6):414–420.
  44. Matsuoka K, et al. Low-dose interleukin-2 therapy restores regulatory T cell homeostasis in patients with chronic graft-versus-host disease. *Sci Transl Med*. 2013;5(179):179ra143.
  45. Koreth J, et al. Interleukin-2 and regulatory T cells in graft-versus-host disease. *N Engl J Med*. 2011;365(22):2055–2066.
  46. Martino M, et al. Extracorporeal photopheresis, a therapeutic option for cutaneous T-cell lymphoma and immunological diseases: state of the art. *Expert Opin Biol Ther*. 2012;12(8):1017–1030.
  47. Wolff D, et al. Consensus conference on clinical practice in chronic GVHD: second-line treatment of chronic graft-versus-host disease. *Biol Blood Marrow Transplant*. 2011;17(1):1–17.
  48. Furlong T, et al. Therapy with mycophenolate mofetil for refractory acute and chronic GVHD. *Bone Marrow Transplant*. 2009;44(11):739–748.
  49. Apisarnthanarax N, et al. Extracorporeal photopheresis therapy in the management of steroid-refractory or steroid-dependent cutaneous chronic graft-versus-host disease after allogeneic stem cell transplantation: feasibility and results. *Bone Marrow Transplant*. 2003;31(6):459–465.
  50. Couriel DR, et al. Sirolimus in combination with tacrolimus and corticosteroids for the treatment of resistant chronic graft-versus-host disease. *Br J Haematol*. 2005;130(3):409–417.
  51. Johnston LJ, et al. Rapamycin (sirolimus) for treatment of chronic graft-versus-host disease. *Biol Blood Marrow Transplant*. 2005;11(1):47–55.
  52. Olivieri A, et al. Imatinib for refractory chronic graft-versus-host disease with fibrotic features. *Blood*. 2009;114(3):709–718.
  53. Inamoto Y, et al. Failure-free survival after second-line systemic treatment of chronic graft-versus-host disease. *Blood*. 2013;121(12):2340–2346.
  54. Vogl UM, et al. Lung transplantation for bronchiolitis obliterans after allogeneic hematopoietic stem cell transplantation: a single-center experience. *Transplantation*. 2013;95(4):623–628.
  55. Rabitsch W, et al. Successful lung transplantation for bronchiolitis obliterans after allogeneic marrow transplantation. *Transplantation*. 2001;71(9):1341–1343.
  56. Woyach JA, et al. Bruton's tyrosine kinase (BTK) function is important to the development and expansion of chronic lymphocytic leukemia (CLL). *Blood*. 2014;123(8):1207–1213.
  57. Rushworth SA, Murray MY, Zaitseva L, Bowles KM, MacEwan DJ. Identification of Bruton's tyrosine kinase as a therapeutic target in acute myeloid leukemia. *Blood*. 2014;123(8):1229–1238.
  58. Atherly LO, Lucas JA, Felices M, Yin CC, Reiner SL, Berg LJ. The Tec family tyrosine kinases Itk and Rlk regulate the development of conventional CD8<sup>+</sup> T cells. *Immunity*. 2006;25(1):79–91.
  59. Blazar BR, Taylor PA, Panoskaltis-Mortari A, Vallera DA. Rapamycin inhibits the generation of graft-versus-host disease- and graft-versus-leukemia-causing T cells by interfering with the production of Th1 or Th1 cytotoxic cytokines. *J Immunol*. 1998;160(11):5355–5365.
  60. Blazar BR, et al. Engraftment of severe combined immune deficient mice receiving allogeneic bone marrow via in utero or postnatal transfer. *Blood*. 1998;92(10):3949–3959.
  61. Lapalombella R, et al. Tetraspanin CD37 directly mediates transduction of survival and apoptotic signals. *Cancer Cell*. 2012;21(5):694–708.